Preparation of Polypropylene/Montmorillonite Nanocomposites with an Exfoliated Structure by a Designed Route

Haoqun Hong, Hui He, Zhixin Jia, Chao Ding, Demin Jia

College of Materials Science and Engineering, South China University of Technology, Guangzhou 510640, People's Republic of China

Received 15 July 2005; accepted 27 December 2005
DOI 10.1002/app.24134
Published online in Wiley InterScience (www.interscience.wiley.com).

ABSTRACT: Nanocomposites of polypropylene (PP) and montmorillonites (MMT) were prepared by solid-phase grafting reactive organomontmorillonite (ROMT) and polar monomers onto powdered PP and melt-blending granule PP with the master batches as PP/MMT grafting copolymers (PPMG). The structure and properties of the PP/MMT nanocomposites (PPMN) were investigated by gel permeation chromatography (GPC), Fourier transform infrared spectroscopy (FTIR), X-ray diffraction (XRD) patterns, transmission electron microscopy (TEM), dynamic mechanical analysis, differential scanning calorimetry, and thermogravimetric analysis. GPC showed that the numerical molecular weight and polydispersity of the graft copolymers of PPMG were approximately 4793 and 2.197, respectively. FTIR confirmed the solid-phase graft copolymerization. XRD and TEM indicated the formation of the exfoliated, layered silicates (tactoids). The mole ratio of compound alkylammoniums and the exothermic enthalpy from solid-phase graft copolymerization played key roles in the formation of tactoids. The optimum mole ratio of organophilic alkylammonium to reactive alkylammonium was 3 : 1. The mechanical and thermal properties increased with the contents of PPMG, and a preferable state was achieved at approximately 8 phr PPMG (parts of reagent per 100 parts of PP) because of the plastification of the exfoliated silicates and the graft copolymers. © 2006 Wiley Periodicals, Inc. J Appl Polym Sci 102: 3889–3899, 2006

Key words: poly(propylene) (PP); organoclay; solid phase graft copolymerization; nanocomposites

INTRODUCTION

Recently, there has been great interest in polymer/clay nanocomposites because of their high performance at quite low loadings compared to that with conventional filled-polymer composites.[1–7] MMT, with a layered structure of a high aspect ratio,[8] is one of the most important clays for preparing polymer/clay nanocomposites because of its abundant supply and low cost. Common polymer/clay nanocomposites start with the preparation of the organophilic clays with organic cations such as alkylammoniums and aminophenols in exchange with interlayer sodium cations in order to reduce the surface energy to facilitate the intercalation of macromolecule chains into the clay interlayers. However, it is difficult for polyolefins to form an ideal intercalated structure with organophilic clays because the polyolefins are highly hydrophobic and, if any nanocomposites form, they are still thermally unstable.[9] Therefore, it is important to enhance the interaction between clays and polyolefins by compatibilizers such as graft copolymers,[10,11] or by introducing initiators[12] or reactive groups[13] into the clay interlayers to form a stable intercalated structure.

Graft copolymers are one of the excellent compatibilizers for polymer/clay nanocomposites. The major methods of synthesizing graft copolymers are melting graft copolymerization, solution graft copolymerization, radiation graft copolymerization, and solid-phase graft copolymerization. Compared to the other graft methods, solid-phase graft copolymerization has the advantages of using a lower reaction temperature and having fewer side reactions, less solvent pollution, and simple postprocessing. Solid-phase graft copolymerization was first reported by Canterino[14] in the 1960s, and recently has seen rapid development of its use. Monomers used for solid-phase graft copolymerization include maleic anhydride (MAH), styrene (St), methyl methacrylate (MMA), and butyl acrylate (BA). The most commonly used monomer is MAH because it is highly hydrophilic and easily obtained. But graft copolymers such as PP graft MAH have the disadvantages of difficult homopolymerization, low graft efficiency, easy sublimation, and causing environmental pollution. Recently, some researchers has developed multiple-monomer solid-phase graft

Correspondence to: Hui He (pshuihe@scut.edu.cn).
Contract grant sponsor: National Natural Science Foundation of China; contract grant number: 20304003.
Contract grant sponsor: Guangdong Natural Science Foundation of China; contract grant number: 020966, 039172.

copolymers.[15–19] Among them, Jia et al. investigated solid-phase grafting of ternary monomers onto PP. The ternary graft copolymers of PP have the characteristics of high graft efficiency, long side chains, and an adjustable side chain structure, and they show improved compatibilization in PP composites and blends.[15–17]

In the present work, we attempted to join ROMT in solid-phase graft copolymerization and simultaneously make ternary monomers *in situ* from the grafted copolymers in order to stabilize the intercalated structure of MMT and to achieve a stable exfoliated structure step by step during the preparation of ROMT, PPMG, and PPMN. To attain the desired structure, a preparation route was designed, as displayed in Figure 1. Cetyltrimethyl ammonium bromide (CTAB), a highly organophilic alkylammonium, and dimethyl diallyl ammonium chloride (DMDAAC), a reactive alkylammonium, were the compound alkylammoniums used in the preparation of ROMT, as shown in Figure 1(a). At this stage, the interlayer space of MMT was expanded beyond 2.0 nm due to the change of entropy inside interlayers. ROMT, MAH, MMA, and BA were initiated together by benzoyl peroxide (BPO) to copolymerize and graft onto PP in solid phase in order to synthesize PPMG, as shown in Figure 1(b). During the solid-phase graft copolymerization, the interlayer space escalated beyond 4.0 nm by the exothermic enthalpy from the solid-phase graft copolymerization. Compatibilizers were *in situ* formed by solid-phase grafting the ternary monomers onto PP. Finally, the PPMG was melt-blended with PP to prepare the exfoliated PPMN. In the melt blending stage, the interlayers of MMT provided sufficient space for PP to further intercalate. As a result, the intercalated silicates were gradually exfoliated into tactoids by shearing strength, as shown in Figure 1(c).

EXPERIMENTAL

Materials

Granulated PP and powdered PP (F401, MFI = 3.172 g/min) were supplied by Guangzhou Yinzhu Group Inc. Na^+-MMT with a cation-exchange capacity (CEC) of 100 mequiv/100 g, was purchased from Guangdong Nanhai Nonmetal Co., Ltd. The MAH, which was AR grade, was ground before use. MMA and BA, both AR grade, were extracted with a 0.1 mol/L NaOH solution to remove the inhibitor, then washed with distilled water and dried by a molecular sieve before use. AR-grade BPO was dissolved in methenyl chloride, precipitated with methanol, and dried in a vacuum desiccator after filtration. AR-grade CTAB was purchased from Shanghai Bio Life Science & Technology Co., Ltd., and used as received. AR-grade DMDAAC was obtained from Guangzhou Shuangjian Chemical Commerce Co., Ltd.

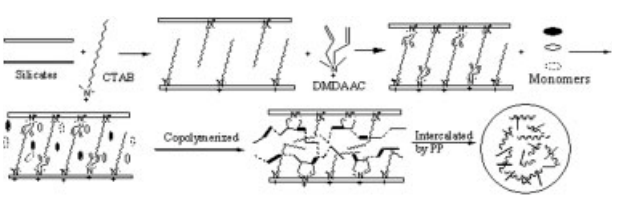

Figure 1 Scheme of PPMN formation process by MMT compound organification.

Preparation of PP/MMT nanocomposites

Different mole ratios of CTAB and DMDAAC were weighed for cation exchange based on the CEC of MMT and confected into a 1 mol/L water solution. Then 100 g of MMT was dissolved in 1000 mL of distilled water under stirring. The temperature of the MMT suspension was raised to 80°C. The CTAB solution was dripped into the suspension through a filler to react with the interlayer Na^+ for a specified time. Then the DMDAAC solution was dripped into the suspension. The ROMT was filtrated and washed with distilled water until no haloid ion was detected by silver nitrate after ion exchange. After the ROMT was dried to a constant weight at 60°C, it was sifted with a 300-mesh sieve. Solid-phase graft copolymerization was carried out as described in the literature.[17] The powdered PP, xylene, ROMT, polar monomers, and BPO were successively added to a stainless-steel reactor to react under a nitrogen atmosphere for a specified time at a specified temperature. The PPMG contained approximately 40 wt % MMT, as measured by thermogravimetric analysis (TGA). The reaction products were washed with hot water, dried at 60°C to a constant weight to get PPMG. PP, the stabilizer, and different loadings of PPMG were premixed in a tumbling mixer, melt-blended in a rotating twin-screw extruder, and injected into an injection molder. The injected samples were cooled at room temperature for 24 h before testing.

Measurements

GPC was carried out on a Waters GPC instrument with polystyrene as calibration curves. The graft copolymers used for GPC analysis were extracted by acetone in a Soxhlet extractor for 24 h. The acetone solution was air-dried and evaporated in a vacuum desiccator in order to obtain the extractives, which contained the ternary oligomers, and a small quantity of acetone and monomers. To reflect the real molecular-weight distribution, the extractives were not further purified. The solvent used for the extractives was tetrahydrofuran (THF).

FTIR was performed on a Nicolet 710 FTIR spectrometer to confirm that ROMT had taken part in the solid-phase graft copolymerization. PPMG was ground with a mortar, sieved with a 50-mesh sieve, washed with water, and extracted with acetone in order to remove the ungrafted oligomers. The disposed PPMG was boiled in xylene at 130°C to remove the ungrafted PP and reboiled for 3 time to clear the ungrafted PP. The deposit was washed with acetone and dried until it was a constant weight. It was compression-molded into tablets with KBr before test.

X-ray diffraction (XRD) patterns were obtained with D/MMAX-III XRD equipment equipped with the Cu Kα radiation. The scanning angle was 1°–50°, and the scanning rate was 12°/min.

FEI TECNAI G_2 transmission electron microscopy (TEM) was used to study the morphology of the specimens after being sliced into ultrathin slices.

Tensile testing and flexural testing were performed with a universal testing machine (DCS-5000, Shimadzu) at room temperature according to ISO Standards 5427-2 (1993) and 178 (1993), respectively. Notched impact testing was performed according to ISO Standard 180 (1993).

Melt flow rate (MFR) was measured with XNR-400 III MFR equipment. The test temperature was 230°C, and compression weight loading was 2.16 kg.

Dynamic mechanical analysis (DMA) was carried out on a TA 2980 in a single cantilever mode. Testing frequency was 1 Hz, and the heating rate was 3°C/min.

Differential scanning calorimetry (DSC) was performed with a TA DSC 2910 by heating the sample to 200°C at a calefactive rate of 20°C/min, maintained for 10 min to avoid the therm history, cooling to 40°C (with 2 min of equilibration at 40°C), and reheating to 200°C at constant rates of 5°C, 10°C, 20°C, 30°C, and 40°C/min. Exothermic and endothermic flows were recorded as a function of temperature. Crystallinity (%) was calculated on the basis of endothermic enthalpy (ΔH_f) as $\Delta H_f^*/\Delta H_f^0$. ΔH_f^* was the endothermic enthalpy of the samples. ΔH_f^0 (= 165 J/g) was the endothermic enthalpy of PP at 100% crystallinity.[20]

TGA was performed with a TA TGA 2050 instrument by heating the sample to 600°C at a calefactive rate of 20°C/min. Percentage of weight loss was recorded as a function of temperature. The amount of MMT in PPMN also was confirmed by TGA.

RESULTS AND DISCUSSION

FTIR analysis

As shown in Figure 2, the spectra of PPMG were similar to the spectra superimposed by ROMT and PP. The characteristic peaks at 1363 and 1475 cm^{-1} were ascribed to the bending vibrations of methyl and methylene of PP. The characteristic peaks at 2854–2926 cm^{-1} were ascribed to the stretch vibrations of methyl, methylene, and methyne of PP.[21] However, because the alkyls in CTAB and DMDAAC might be similarly absorbed to the methyl and methylene of PP, the grafting of PP with MMT could not be confirmed by characteristic peaks at 2854 and 2926 cm^{-1}; instead it was confirmed by characteristic peaks at 1363 cm^{-1} (a new small peak) and 1475 cm^{-1} (increased intensity). The characteristic peak at 1730 cm^{-1} came from the absorption of carbonyl groups of MMA. The characteristic peaks of the other monomers were too weak to be recognized because their proportion was small compared to that of PP and MMT. However, solid-phase graft copolymerization of ternary monomers was demonstrated by Jia et al.[16] From FTIR analysis, it can be concluded that MMT and the monomers really did take part in the solid-phase graft copolymerization.

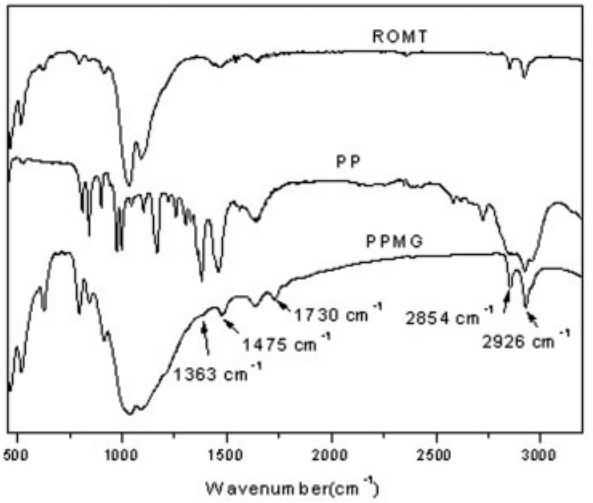

Figure 2 FTIR spectra of ROMT, PP, and PPMG.

Length of the grafted side chains

To investigate the length of the grafted side chains, solid-phase graft copolymerization of MAH/MMA/BA onto PP without MMT (designated as PPTM) was carried out under the same condition as of PPMG. Because of the structural similarity of PPTM and PPMG, GPC was carried out on the extractives of PPTM instead those of PPMG in order to measure the lengths of the grafted side chains. To display the structural similarity of the extractives of PPTM and the grafted side chains of PPTM, PPTM, and their extractives, they were measured by TGA before GPC measurement.

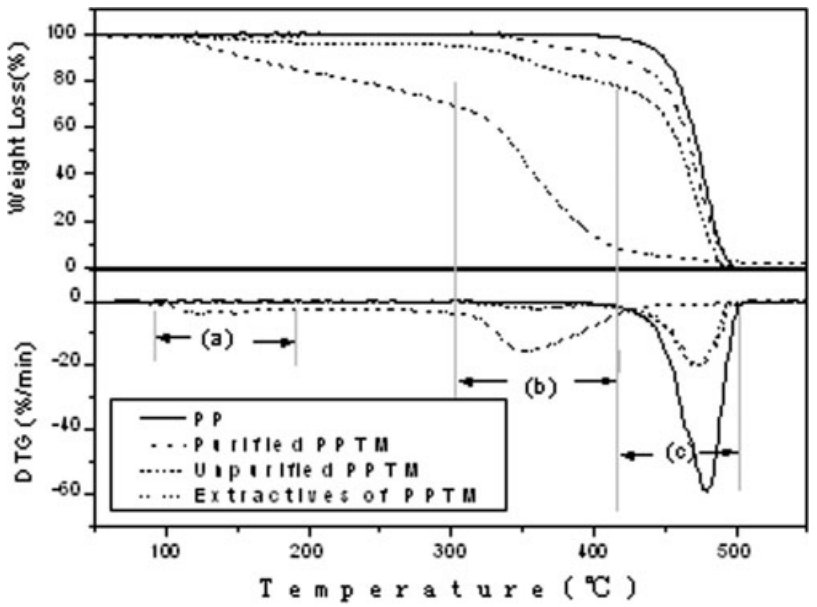

Figure 3 TG and DTG curves of PPTM and its extractives.

Free radicals were considered to have initiated the graft copolymerization as well as the ungraft copolymerization of the monomers.[22–24] This implies that the ungrafted oligomers had a reaction mechanism, structure, and properties that were similar to those of the grafted side chains. Provided that the grafted side chains had a structure and properties similar to those of the ungrafted oligomers, they should have had a similar extent of temperature of weight loss. As shown in Figure 3, Region (a) was approximately from 85°C to 180°C, whereas the residues of the monomers and acetone and the oligomers of lower molecular weight in the extractives degraded. But the lower-molecular-weight oligomers in the extracted PPTM were too small to be distinguished. Region (b) was approximately from 300°C to 380°C, where most of the ungrafted oligomers and the grafted side chains on the PP matrix degraded. This indicated the ungrafted oligomers really had a temperature of the extent of weight loss similar to that of the graft side chains. Therefore, the length of the grafted side chains would be displayed by that of the ungrafted oligomers. In addition, the degree of graft of PPTM was indicated by the weight loss in Region (b) of 9.6%. Region (c) went from approximately 380°C to 500°C, which had the most degradation of PP matrix. It was shown that the grafted side chains were long enough to be detected in the TGA curves. Graft side chain length was confirmed by GPC.

As shown in Table I, the GPC results indicated that the number-average molecular weight, weight-average molecular weight, and molecular weight distribution of the grafted side chains were 4793, 10,529, and 2197, respectively.

XRD patterns of MMT

The idea about the preparation of organo-MMT by compound alkylammoniums derived from the unsatisfied result of the organo-MMT being preparedn only by DMDAAC, that is, CTAB : DMDAAC of 0 : 1. DMDAAC has two double bonds that are prone to react mutually and form a penta-annulet.[25] Moreover, the molecular chains of the DMDAAC are too short to make MMT effectively organophilic. When MMT was modified just by DMDAAC, the double bonds embedded in the interlayers of MMT reacted with each other. As a result, melt blending could not further expand the interlayers of MMT. As shown in Table II, the X-ray peak (d_{001}) increased from 1.24 nm of pristine MMT to 1.45 nm of ROMT. But it remained at 1.47 nm for PPMG and PPMN, indicating that the reactive groups had reacted with each other during the solid-phase graft copolymerization.

However, compound organopreparation had a dramatic effect on the expansion of the MMT interlayer space. Figure 4 shows the XRD patterns of compound modified organo-MMT (CTAB : DMDAAC = 3 : 1)

TABLE I
GPC Parameters of PPTM

Sample	M_n	M_w	Polydispersity	MP	Retention time	Start time	End time	Area
PPTM	4793	10,529	2.197	9987	26.877	23.700	30.683	3,758,77

TABLE II
Interlayer Space (*d*001) change of MMT in Different Products Modified by Different Mol Ratios of Compound Alkylammoniums

CTAB : DMDAAC	Pristine MMT	ROMT	PPMG (40 wt % MMT)	PPMN (8 phr PPMG)
0 : 1	1.24	1.45	1.47	1.47
1 : 1	1.24	2.09	4.37	—
2 : 1	1.24	2.18	4.51	—
3 : 1	1.24	2.24	4.60	—
4 : 1	1.24	2.12	3.42	3.53

Note: Three significant figures are shown for the results of the interlayer space.

during the preparation of PPMN. Obviously, the X-ray peak (d_{001}) shifted to a small angle through organopreparation, graft copolymerization and intercalation. The interlayer space of MMT was expanded from 1.24 nm of pristine clay to 2.24 nm of ROMT and then to 4.60 nm of PPMG. No obvious diffracting peak was identified after melt blending, indicating the formation of the exfoliated structure. The small peaks at 1.24 nm for ROMT and PPMG were the characteristic peaks of DMDAAC. They were assigned to little MMT that was single-modified by DMDAAC during compound modification, but they did not affect the further expansion of the interlayer space.

To understand whether solid-phase graft copolymerization and organopreparation really did affect the intercalation, change in the XRD patterns was investigated for other compound systems (that is, CTAB : DMDAAC = 1 : 1, 2 : 1, and 4 : 1). As shown in Table II, similar results were obtained in the 1 : 1 and 2 : 1 compound systems. However, the interlayer space in the 4 : 1 compound system was only 3.53 nm, even after melt blending. It seems that the 3 : 1 compound system had a better-intercalated structure than the others. Several reasons explain this distinct modification.[26–28] First, when CTAB was used to modify MMT, its chain segments were long enough to prevent the mutual reaction of the double bonds of DMDAAC and make MMT highly organophilic. Second, when DMDAAC modified the silicates after CTAB, it led to the crowding of the interlayers and destroyed the tactic arrangement of CTAB in the MMT interlayers. According to the thermodynamics of polymer intercalation into layered silicates, the molecular chains tended to exclude each other to reduce the entropy, leading to the expansion of the interlayer space. So even in ROMT, the interlayer space of some silicates was larger than 4.00 nm after two steps of organopreparation, as shown in Figure 4. In the 4 : 1 compound system, the number of double bonds did not have enough force to expand the MMT interlayer space. Third, during the solid-phase graft copolymerization, the thermal energy absorbed from outside and the exothermic enthalpy from the graft reaction could overcome the reduction of entropy, which caused the interlayer space to be expanded further. During melt blending, the interlayer space was large enough for the PP matrix to intercalate sufficiently. Naturally, the silicates were exfoliated and uniformly dispersed. In addition, it had been reported that the intercalated molecular chains of PP matrix were prone to be excluded from the interlayers of MMT because these nanocomposites were thermally unstable.[9] But the organoprepared PP/MMT system compound was more stable because MMT took part in the solid-phase graft copolymerization and *in situ*–formed compatibilizers.

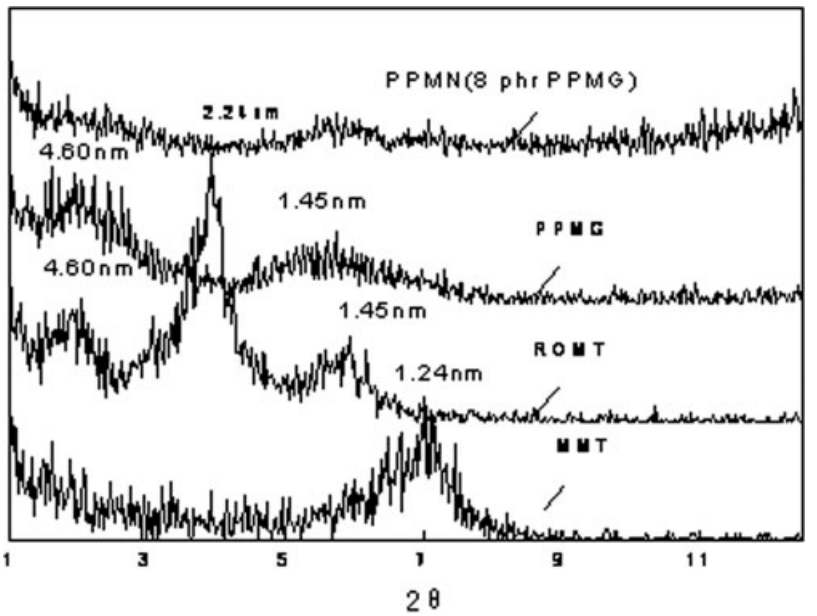

Figure 4 Comparison of XRD patterns of MMT interlayer space (CTAB:DMDAAC = 3 : 1).

TEM characteristics of PPMN

Figure 5 compares two TEM images of different magnifications in order to display the state of dispersion of the exfoliated stacks (tactoids), as illustrated by the 3 : 1 compound system. The dark agglomerates are the cross sections of the tactoids and the dark dots the cross sections of the exfoliated silicates, as shown in Figure 5(a). Obviously, most silicates were uniformly dispersed into tactoids, and some of the exfoliated silicates were well dispersed at the nanometer level in the PP matrix. Figure 5(b) shows an image shot at an of the tactoids in which the dark flakes are the oblique sections of the exfoliated silicates. It reveals that even in the tactoids the silicates were partly exfoliated. Figure 6 shows the TEM images of PPMN prepared with different alkylammonium compounds in which the dark lines are the cross sections of the tactoids. The size of the tactoids was associated with the mole ratio of CTAB to DMDAAC. It appears that the dispersion of the silicates increased as the mole ratio of CTAB to DMDAAC was increased. The mean size of the dispersed tactoids of the 3 : 1 compound system was smaller than that of the other systems. However, the mean size of the aggregates of the 4 : 1 compound system increased, indicating more silicates were not sufficiently exfoliated. This was consistent with the XRD results.

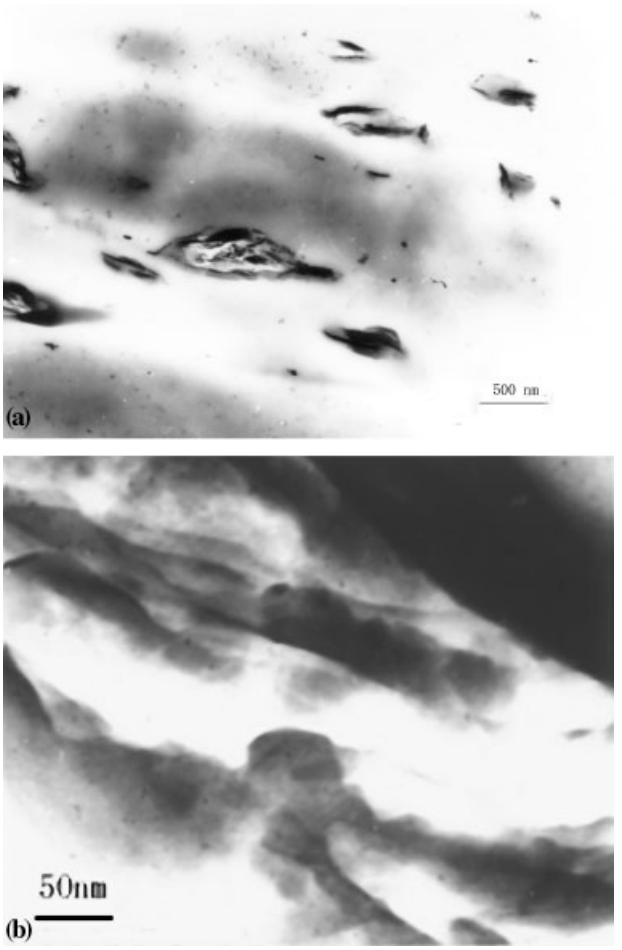

Figure 5 TEM images of the dispersed tactoids of the 3 : 1 compound system (8 phr PPMG): (a) 500 nm, (b) 50 nm.

Mechanical properties

Table III presents the mechanical properties of PPMN. In the four compound systems under investigation, the mechanical properties increased with the addition of PPMG. Obviously, the mechanical properties were preferable when the content of PPMG was approximately 8 phr and remained stable with more loadings of PPMG, shown by the numbers in boldface in Table III. Comparing the four compound systems, it seems that the 3 : 1 system performed the best and the 4 : 1 compound system performed the worst at any PPMG content. The mechanical properties of the 3 : 1 compound system with 8 phr PPMG were much better than those of the other compound systems. The tensile strength, flexural strength, flexural modulus, and notched impact strength of the 3 : 1 system with 8 phr PPMG were 35.8 MPa, 75.8 MPa, 2425 MPa, and 5.34 kJ/m^2, respectively. This indicates the 3 : 1 compound system had a better intercalated structure and thus performed better than the other compound systems. The inferior properties of the 4 : 1 system were attributed to the insufficient intercalation of the clay interlayers, as discussed above.

MFR of PP and PPMN

Table IV shows the MFR of the four compound systems as a function of MMT. Obviously, MFR increased with the addition of PPMG for any compound system. The preferable MFR was attained when 8 phr PPMG was added, but additional loadings of MMT did not cause the MFR to increase. The 3 : 1 compound system exhibited better flow properties that might be suitable for a composite process. This implied the silicate exfoliation in the PP matrix was valid because the exfoliated silicates and the graft copolymers acted as excellent plasticizers.[29,30]

DMA measurements

Because the 3 : 1 CTAB : DMDAAC compound system performed better, the following property analysis was just carried out on the 3 : 1 system. DMA at a fixed frequency (1Hz) was operated from $-40^{\circ}C$ to $100^{\circ}C$. Storage modulus (E'), dynamic loss modulus (E''), and loss factor (tan δ) as a function of temperature were plotted and are shown in Figure 7. Storage modulus [Fig. 7(a)], and loss modulus of PP [Fig. 7(b)] dramatically increased with the addition of PPMG. This was

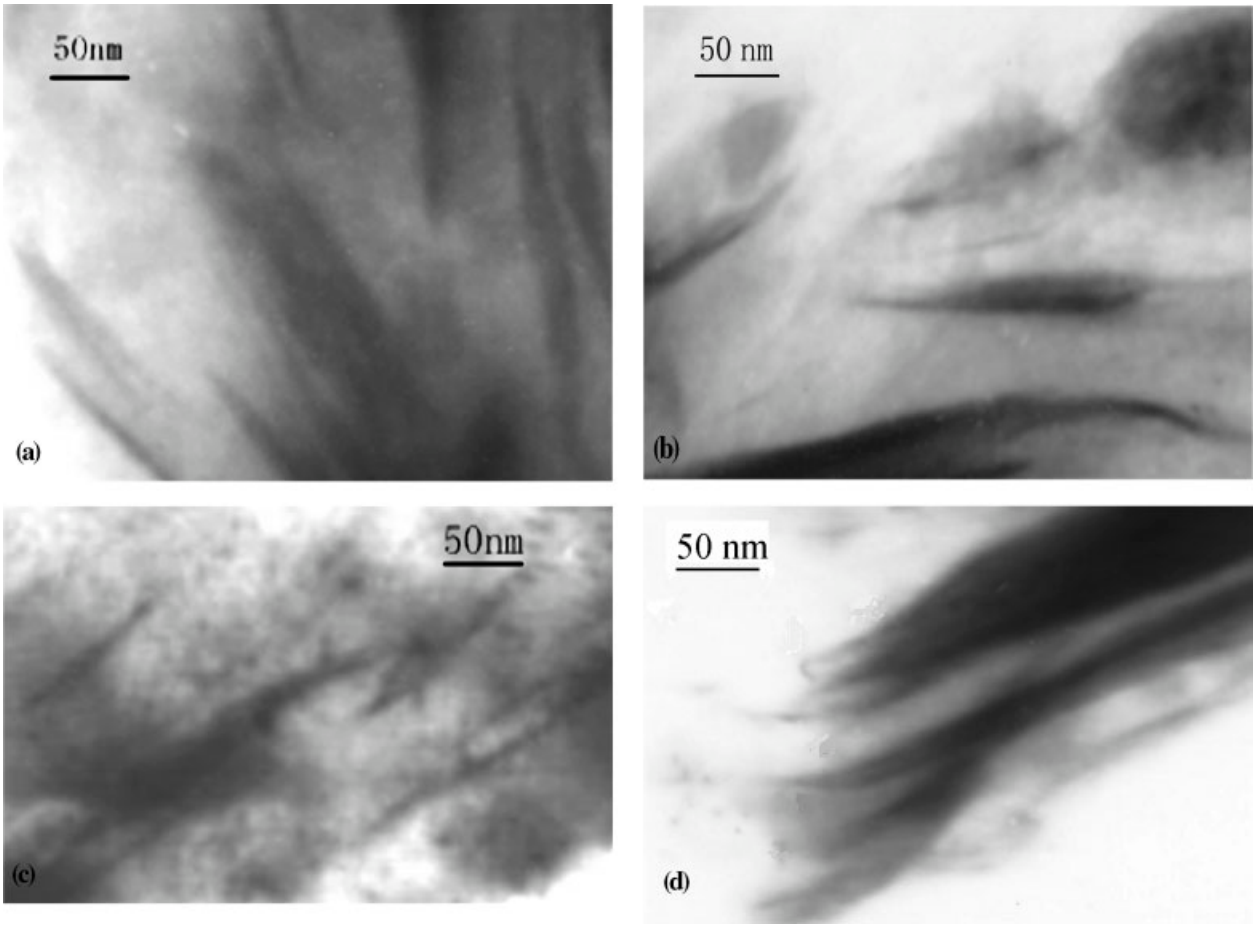

Figure 6 TEM images of of PPMN (8 phr PPMG) with different mole ratios of the compound alkylammoniums (50 nm): (a) 3 : 1 CTAB : DMDAAC, (b) 2 : 1 CTAB : DMDAAC, (c) 3 : 1 CTAB : DMDAAC, (d) 4 : 1 CTAB : DMDAAC.

TABLE III
Effect of PPMG on Mechanical Properties of PPMN

		PP	PPMN1	PPMN2	PPMN3	PPMN4	PPMN5
Sample PPMG (phr)		0	2	4	6	8	10
Tensile strength (MPa)	1 : 1	25.6	31.3	32.4	33.2	**34.2**	34.1
	2 : 1	25.6	31.9	32.7	33.9	**34.7**	33.9
	3 : 1	25.6	33.8	34.7	35.2	**35.8**	35.4
	4 : 1	25.6	30.3	31.2	32.6	**33.3**	33.0
Flexural strength (MPa)	1 : 1	57.0	61.3	64.0	65.7	**71.0**	70.5
	2 : 1	57.0	63.9	66.7	69.0	**71.6**	71.1
	3 : 1	57.0	65.0	68.9	72.7	**75.8**	75.4
	4 : 1	57.0	60.2	62.1	63.3	**65.3**	64.5
Flexural modulus (MPa)	1 : 1	1257	1860	2042	2161	**2201**	2190
	2 : 1	1257	1988	2148	2226	**2329**	2293
	3 : 1	1257	2002	2265	2358	**2425**	2418
	4 : 1	1257	1798	1854	1915	**1984**	1968
Notched impact strength (kJ/m^2)	1 : 1	3.01	4.15	4.30	4.54	**4.64**	4.59
	2 : 1	3.01	4.20	4.51	4.71	**4.82**	4.80
	3 : 1	3.01	4.49	4.85	5.08	**5.34**	5.30
	4 : 1	3.01	4.06	4.19	4.38	**4.42**	4.37

Note: The results of the mechanical tests are shown with three significant figures, except for the results of flexural modulus, which give four significant figures.

TABLE IV
MFR (g/10 min) Data of PP and PPMN Containing Various Concentrations of PPMG

		CTAB : DMDAAC			
Sample	PPMG (phr)	1 : 1	2 : 1	3 : 1	4 : 1
PP	0	3.17	3.17	3.17	3.17
PPMN1	2	3.08	3.18	3.69	3.24
PPMN2	4	3.42	3.25	4.14	3.54
PPMN3	6	4.18	3.93	4.92	3.64
PPMN4	8	4.49	3.85	4.88	3.47
PPMN5	10	4.35	3.79	4.84	3.52

Note: Four significant figures are given for the MFR results.

consistent with the report of Alexandre et al.[31] Small amounts of MMT with a high aspect ratio were enough to improve the mechanical properties when silicates were intercalated by PP and to be uniformly dispersed in PP matrix. However, the dynamic mechanical properties did not increase in proportion to the additions of PPMG. It attained its optimum state when PPMG reached 8 phr. It is interesting that T_g of PPMN was lower than that of PP, as shown in [Fig. 7(c)].

The reason the mechanical properties and DMA had a preferable state was that the graft copolymers acted as not only as interfacial modifiers but also as plastifiers of PPMN.[29] Khunova reported that graft copolymers of PP acted as ''diluents of viscosity'' to plastify the PP matrix as well as interfacial modifiers in order to enhance the interfacial interaction in PP/inorganic filler composites.[30] In a system of low filler loadings, the graft copolymers acted more as diluents of viscosity than interfacial modifiers. In a system with high filler loadings, however, the graft copolymers acted more as interfacial modifiers than as diluents of viscosity. Meanwhile, the more graft copolymers were added, the more oligomers were introduced. This made the plastification of graft copolymers overtake interfacial modification. As for polymer/clay nanocomposites, the filler loadings were generally less than 10 wt %. The oligomers acted more as diluents of viscosity than as interfacial modifiers of PPMN. This was also the reason why the T_g of PPMN was lower than that of PP. Meanwhile, when more PPMG was loaded, the dispersed silicates tended to agglomerate, resulting in the deterioration of the properties of PPMN.[16] Therefore, the properties tended to be in a preferable state at 8 phr PPMG.

DSC measurements

Clay can help to improve the thermal properties and enhance the heterocrystallization of polymer/clay nanocomposites.[32] And it may cause a β crystal to form. No β-crystal was discovered with low loadings of PPMG. But a β-crystal appeared near 145°C, when more than 4 phr PPMG was added, as shown by the arrows in Figure 8. The DSC results are listed in Table V. The top melting point of PPMN in the investigation was 166.2°C at 10 phr PPMG.

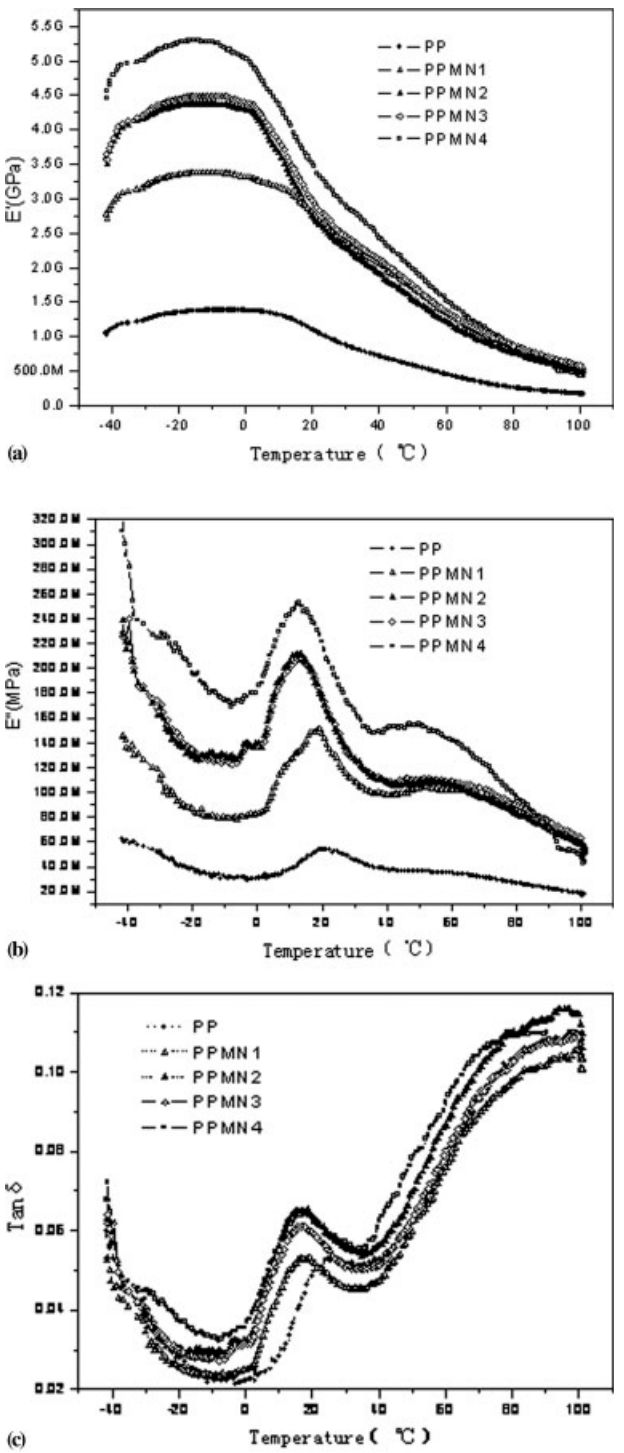

Figure 7 DMA spectra of PPMN (CTAB:DMDAAC = 3 : 1): (a) storage modulus, (b) loss modulus, (c) loss factor. PPMN1 contained 4 phr PPMG, PPMN2 6 phr PPMG, PPMN3 8 phr PPMG, and PPMN4 10 phr PPMG.

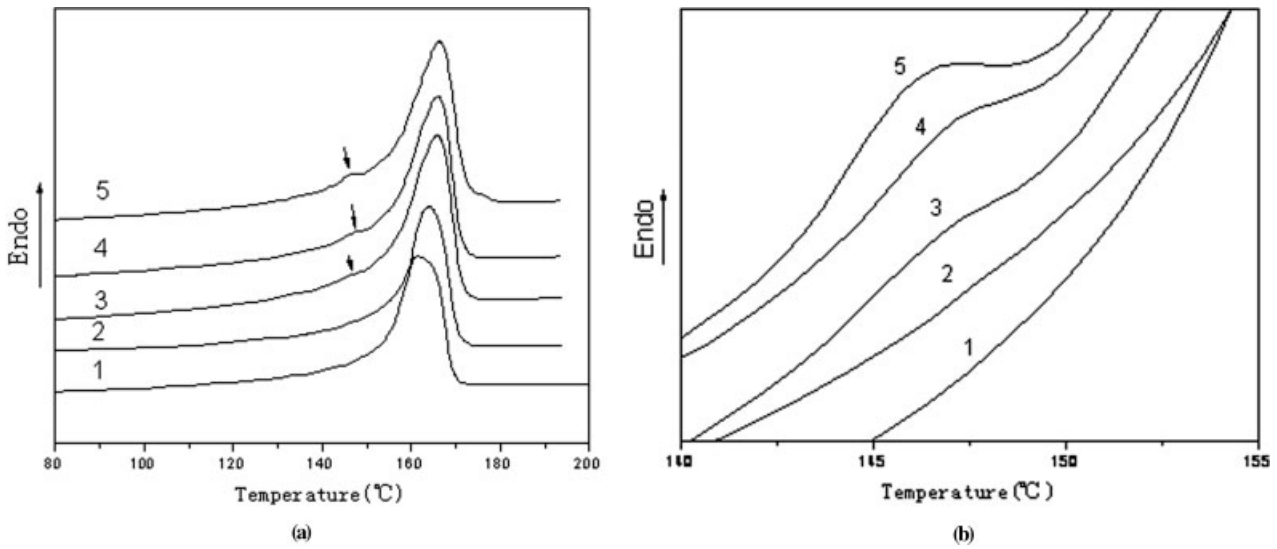

Figure 8 Comparison of DSC curves of PP and PPMN (CTAB:DMDAAC = 3 : 1) in (a) a wide temperature range and (b) in the β-crystal temperature range: (1) PP, (2) PPMN1 (4 phr PPMG), (3) PPMN2 (6 phr PPMG), (4) PPMN3 (8 phr PPMG), (5) PPMN4 (10 phr PPMG).

Meanwhile, the crystallinity of PPMN increased with PPMG content, from 40.69% PP to 49.94% at 8 phr PPMG and remained stable with additional increases in PPMG.

As can be seen from Figure 9, heat flow increased when it was cooled at growing speed, which meant the crystallization of PP was more sufficient when cooling occurred more slowly because the molecular chains had enough time to arrange integrally. But when rate of cooling decreased to 5°C/min and 10°C/min, the two exothermic curves of PP and PPMN overlapped. This meant the movement of PP chains might have been enhanced by the exfoliated MMT and the graft copolymers, and the PP chains had sufficient time to rearrange in both PP and PPMN when the speed of cooling was less than 10°C/min. Meanwhile, the crystalline temperature and crystallization enthalpy of PPMN were higher than those of PP at any cooling speed. When the rate of cooling was faster, the difference between the two systems in crystalline temperature was larger, ranging from 2°C to 6°C depending on the cooling speed. This indicated that MMT was able to improve the thermal properties of the PP matrix and enhance its crystallization as well.

Thermogravimetric analysis

Figure 10 shows a comparison of the TGA curves of PP and PPMN containing different concentrations of PPMG. The TGA results are listed in Table VI. The thermal decomposition properties of PPMN increased with the addition of PPMG. The temperatures of the extrapolated initial decomposition and loss of half the weight of PPMN were higher than those of PP. The temperature of extrapolated initial decomposition increased from 392.3°C for PP to 423.3°C for PPMN2 with 6 phr PPMG loadings. Additional PPMG did not enhance the thermal properties. The temperature of loss of half the weight increased with the PPMG loadings, reaching a maximum with 8 phr PPMG loadings. However, the other decomposing temperatures did not increase. This was attributed to the oligomers built by the polar monomers during solid-phase graft copolymerization, which had a low decomposing temperature compared to that of the PP matrix, as shown in Figure 3. In addition, the weight percentage of the residues represented the virtual content of clay. As calculated from the results shown in Table VI, PPMG contained approximate 40 wt % MMT, as did the other compound systems.

TABLE V
Summary of DSC Results for PP and PPMN (CTAB:DMDAAC = 3 : 1) Containing Various Concentrations of PPMG

Sample	PPMG (phr)	MMT (wt %)	T_m (°C)	ΔH_f^* (J/g)	Crystallinity (%)
PP	0	0	161.4	76.50	46.36
PPMN1	4	1.7	164.0	80.90	49.03
PPMN2	6	2.4	165.8	89.34	54.15
PPMN3	8	3.2	165.9	93.88	56.89
PPMN4	10	4.5	166.2	92.82	56.25

Note: The DSC results are given to four significant figures except for the MMT content, given to two significant figures.

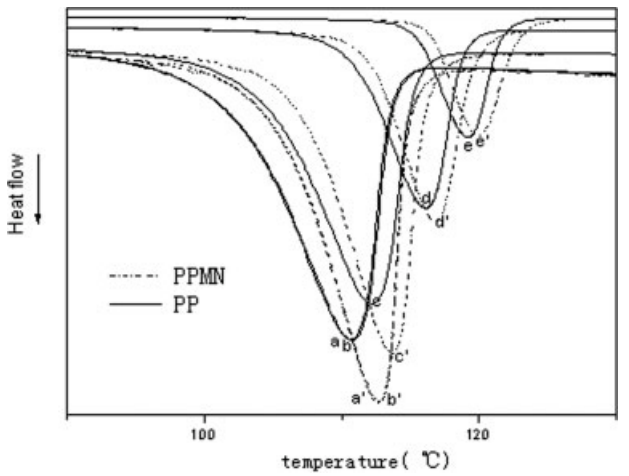

Figure 9 Effect of cooling speed on crystallization behavior of PPMN (CTAB : DMDAAC = 3 : 1, 8 phr PPMG): (a and a′) 5°C/min; (b and b′) 10°C/min; (c and c′) 20°C/min; (d and d′) 30°C/min; (e and e′) 40°C/min.

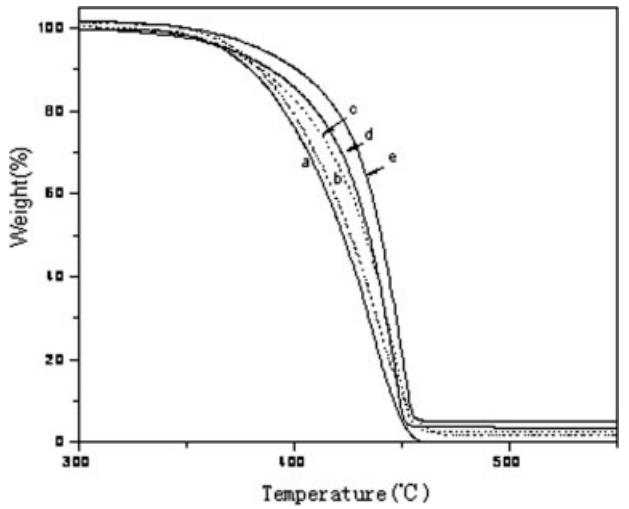

Figure 10 Comparison of TGA curves of PP and PPMN (CTAB : DMDAAC = 3 : 1): (a) PP, (b) PPMN1 (4 phr PPMG), (c) PPMN2 (6 phr PPMG), (d) PPMN3 (8 phr PPMG), (e) PPMN4 (10 phr PPMG).

CONCLUSIONS

A new method has been proposed to prepare PPMN by the solid-phase grafting of ROMT and polar monomers onto PP and melt blending of PP with the master batches, PPMG. Compatibilizers *in situ* formed for polymer and clay during the solid-phase graft copolymerization. FTIR showed that MMT had taken part in the solid-phase graft copolymerization. XRD and TEM showed that the MMT in the 3 : 1 compound system was sufficiently exfoliated and well dispersed in the PP matrix compared to in the other compound systems. But the 4 : 1 compound system had an inferior intercalated structure. The mole ratio of the compound alkylammoniums and exothermic enthalpy from the solid-phase graft copolymerization played key roles in the formation of the exfoliated layered silicates (tactoids). The 3 : 1 compound system had better mechanical, flow, and thermal properties than the other systems. DMA analysis showed that the E' and E'' of the composites were greater than those of PP, but the T_g of PPMN was lower than that of PP in the 3 : 1 compound system. The performance of PPMN improved with the addition of PPMG and reached a preferable state at approximately 8 phr PPMG. DSC analysis demonstrated that MMT could increase the melting point of PPMN and its crystallinity. A β crystal was discovered when more than 6 phr PPMG was added. The nonisothermal crystallization experiment showed that the movement of PP chains was enhanced by the exfoliated MMT and the graft copolymers. PP and PPMN had similar crystal behavior when the rate of cooling was slower than 10°C/min. MMT significantly improved the thermal properties of PPMN, especially at 8 phr PPMN. The reason the properties of PPMN were preferable and the T_g of PPMN was lower than that of PP was that the well-dispersed MMT and the graft copolymers had an effect of plastifying PPMN. Furthermore, the virtual content of MMT in PPMG and PPMN was confirmed by TGA. It was shown that PPMG contained approximately 40 wt % MMT.

TABLE VI
Summary of TGA Results for PP and PPMN (CTAB:DMDAAC = 3 : 1) Containing Various Concentrations of PPMG

Sample	PPMG (phr)	MMT (wt %)	T_{ID} (°C)	T_{EID} (°C)	T_{HW} (°C)	T_{ETT} (°C)	T_{MWL} (°C)
PP	0	0	313.2	392.6	424.9	460.3	473.4
PPMN1	4	1.7	301.5	414.7	432.3	463.3	464.6
PPMN2	6	2.4	299.9	423.6	439.5	458.7	463.3
PPMN3	8	3.2	310.3	417.7	435.3	455.8	464.6
PPMN4	10	4.5	327.9	395.6	424.9	461.7	467.5

Note: T_{ID}, temperature of initial decomposition; T_{EID}, temperature of extrapolated initial decomposition; T_{HW}, temperature of half weight loss; T_{ETT}, temperature of extrapolated termination; T_{MWL}, temperature of maximum weight loss. TGA results are shown to four significant figures, except MMT content, shown to two significant figures.

References

1. Wang, Z. M.; Nakajima, H.; Manias, E.; Chung, T. C. Macromolecules 2005, 36, 8919.
2. Chow, W. S.; Ishak, Z. A. M.; Karger-Kocsis, J.; Apostolov, A. A.; Ishiaku, U. S. Polymer 2003, 44, 7427.
3. Bohning, M.; Goering, H.; Fritz, A.; Brzezinka, K. W.; Turky, G.; Schonhals, A.; Schartel B. Macromolecules 2005, 38, 2764.
4. Merkel, T. C.; He, Z. J.; Pinnau, I.; Freeman, B. D.; Meakin, P.; Hill, A. J. Macromolecules 2003, 36, 6844.
5. Chang, J. H.; An, Y. U. J Polym Sci, Part B: Polym Phys 2002, 40, 670.
6. Hussain, M.; Simon, G. P. J Mater Sci Lett 2003, 22, 1471.
7. Galgali, G.; Agarwal, S.; Lele, A. Polymer 2004, 45, 6059.
8. Shmuel, Y.; Harold, C. Organo-clay Complexes and Interactions. Marcel Dekker: New York, 2002.
9. Strawhecker, K. E.; Manias, E. Chem Mater 2000, 12, 2943.
10. Kim, S. W.; Jo, W. H.; Lee, M. S.; Ko, M. B.; Jho, J. Y. Polymer 2001, 42, 9837.
11. Kawasumi, M.; Hasegawa, N.; Kato, M.; Usuki, A.; Okada, A. Macromolecules 1997, 30, 6333.
12. Wang, X.; Lin, J. J.; Wang, X. Y.; Wang, Z. B. J Appl Polym Sci 2004, 93, 2230.
13. Zhu, J.; Start, P.; Mauritz, K. A.; Wilkie, C. A. Polym Degrad Stabil 2002, 77, 253.
14. Canterino, J. U.S. Pat. 3,162,694 (1964).
15. Jia, D. M.; Luo, Y. F.; Li, Y. M.; Lu, H.; Fu, W. W.; Cheung, W. L. J Appl Polym Sci 2000, 78, 2482.
16. Ding, C.; Jia, D. M.; He, H.; Guo, B. C.; Hong, H. Q. Polym Test 2005, 24, 94.
17. Jia, D. M.; Luo, Y. F.; He, H.; Wang, X. W. (Chinese) Pat. 00,117,390 (2004).
18. Zhang, L. F.; Guo, B. H.; Zhang, Z. M. J Appl Polym Sci 2002, 84, 929.
19. Li, Y.; Xie, X. M.; Guo, B. H. Polymer 2001, 42, 3419.
20. Mark, J. E. Polymer Data Handbook; Oxford University Press: New York, 1999; p 782.
21. Dong, Y. M. Handbook of Polymer Analysis; Sinopec Press: Beijing, 200, p 252.
22. Gaylord, N. G.; Mishra, M. K. J Polym Sci Polym Lett 1983, 21, 23.
23. Shi, D.; Yang, J. H.; Yao, Z. H.; Wang, Y.; Huang, H. L.; Jing, W.; Yin, J. H.; Costa, G. Polymer 2001, 42, 5549.
24. Galia, A.; De Gregorio, R.; Spadaro, G.; Scialdone, O.; Filardo, G. Macromolecules 2004, 37, 4580.
25. Schwarz, H. H.; Lukas, J.; Richau, K. J Membrane Sci 2003, 218, 1.
26. Ray, S. S.; Okamoto, M. Prog Polym Sci 2003, 28, 1539.
27. Wang, X.; Lin, J. J.; Wang, X. Y.; Wang, Z. B. J Appl Polym Sci 2004, 93, 2230.
28. Vaia, R. A.; Giannelis, E. P. Macromolecules 1997, 30, 7990.
29. Wang, D. Y.; Parlow, D.; Yao, Q.; Wilkie, C. A. J Vinyl Addit Technol 2001, 7, 203.
30. Khunova, V.; Zamorsky, Z. Polym Plast Technol 1993, 32, 289.
31. Alexandre, M.; Dubois, P.; Sun, T.; Garces, J. M.; Jerome, R. Polymer 2002, 43, 2123.
32. Liu, X. H.; Wu, Q. J. Polymer 2001, 42, 10013.